Comments on "Direct Atmospheric Forcing of Geostrophic Eddies. Part II: Coherence Maps"

K. H. BRINK AND R. M. SAMELSON

Department of Physical Oceanography, Woods Hole Oceanographic Institution, Woods Hole, Massachusetts

27 January 1997 and 6 August 1997

1. Introduction

Lippert and Müller (1995, henceforth called LM) recently presented a mathematical analysis of the problem of wind stress forcing of current fluctuations below the mixed layer in the open ocean. Their work is a thoughtful and insightful addition to earlier contributions (e.g., Frankignoul and Müller 1979; Brink 1989; Samelson 1989), but there are points of interpretation that deserve comment.

Their model considers barotropic currents and pressure fluctuations forced by a band-limited frequency–wavenumber spectrum of wind stress curl. The results are expressed in terms of energy levels and maps of coherence between current (or pressure) fluctuations at a fixed point (the "mooring" location) and the wind stress curl over an extended area. In many cases, the maximum coherence is with a wind stress curl spatially removed from the measurement site.

The primary mathematical difference between their calculations and those of Brink (1989) and Samelson (1989, 1990) is the structure of the forcing spectrum. Motivated by heavily averaged estimated wind curl autocovariances (e.g., Samelson 1990, Fig. 7), we chose forcing spectra whose transforms (the autocovariances) had no sidelobes. We also used zonally bounded ocean basins, while LM used an infinite ocean with a larger friction coefficient to limit response amplitudes.

The issue we want to raise involves the physical interpretation of results. Brink (1989), for example, explained the theoretical wind–current coherence pattern in terms of forcing and of the group velocities of long and short Rossby waves. This explanation would account, for example, for coherence patterns suggesting zonal currents and pressure being forced by winds to the east of the mooring, and communicated via long Rossby waves. LM apparently reject this argument, stating that "the existence and location of nonlocal or secondary maxima . . . does not reflect nonlocal forcing and energy propagation along wave group trajectories," that "nonlocal maxima are not caused by distant forcing, leading to the awkward notion that variance in the pressure field and velocity field at the same location is generated at different distant locations but represent areas where the phase relation between response and forcing is stable . . . ," and that "no wave groups exist" in their model.

Our first point is that, while LM interpret coherence strictly as a measure of phase stability of one time series relative to another, we assert that the other traditional interpretation (e.g., Bendat and Piersol 1971, p. 142) is also valid: that the coherence is a measure of the "relatedness" of two time series. As such it can suggest cause and effect relations, but with the caveat that high coherence could also depend on a proxy relationship (although a proxy relationship is unlikely in this case, since the wind is unambiguously the forcing agency). To support the viewpoint that the coherence patterns portray causal relations, we provide calculations in section 2 to review the anisotropy of β-plane wind response and in section 3 to show that the model coherence patterns are indeed indicative of where wind forcing of the different variables takes place.

Our second point regards the relevance of the group velocity concept to the mathematics of the problem and to its physical interpretation. We show in section 4 that the group velocity enters this problem in a natural way and that it does provide useful indicators about where observables are forced.

2. Response to isolated forcing

It is instructive to review how the ocean responds to isolated (point) forcing and so to see how information spreads differently for different observables (pressure, east and north velocity). The governing equation for linear, barotropic quasigeostrophic flow in a β-plane ocean with a flat bottom is (e.g., Brink 1989):

Corresponding author address: Dr. K. H. Brink, Department of Physical Oceanography, Woods Hole Oceanographic Institution, Woods Hole, MA 02543.
E-mail: kbrink@whoi.edu

$$\left(\frac{\partial}{\partial t}+\epsilon h^{-1}\right)\left(\frac{\partial^2 p}{\partial x^2}+\frac{\partial^2 p}{\partial y^2}\right)+\beta\frac{\partial p}{\partial x}-\lambda^2\frac{\partial p}{\partial t}=fh^{-1}C, \quad (1)$$

where p is pressure, C the wind stress curl, f the Coriolis parameter, h the water depth, ϵ a bottom resistance parameter, and λ the inverse barotropic Rossby radius of deformation. The (x,y) directions are eastward and northward respectively, and t is time. For the remainder of this section only, we make a rigid-lid assumption, $\lambda = 0$. We seek to review how the ocean responds to a point forcing, so we choose

$$C = b\delta(x)\delta(y)e^{i\omega t}, \quad (2)$$

where δ is the Dirac delta function. It is straightforward to solve (1) using (2) and a Fourier transform in y to obtain an ordinary differential equation in x with the solution:

$$p = \overline{p}(x, y)e^{i\omega t}, \quad (3a)$$

$$\overline{p} = \frac{1}{2\pi}bf(\omega' h)^{-1}\int_{-\infty}^{\infty} e^{-ily}\gamma^{-1}\exp\left\{i[\alpha+\mathrm{sgn}(x)\gamma]\frac{x}{2}\right\}dl, \quad (3b)$$

where the imaginary part of $\gamma > 0$,

$$\gamma = (\beta^2\omega'^{-2} - 4l^2)^{1/2}, \quad (3c)$$

$$\alpha = \beta/\omega', \quad (3d)$$

and

$$\omega' = \omega - i\epsilon h^{-1}. \quad (3e)$$

We evaluated the integral (3b) numerically over the wavenumber range of -10^{-6} cm^{-1} to 10^{-6} cm^{-1} using an adaptive recursive Newton Cotes 8 panel rule (function ''quad8'' of the Matlab© package).

Representative results for pressure and u and v amplitudes are shown in Fig. 1. The eastward (u) and northward velocity components were found using

$$u = -f^{-1}\rho^{-1}\frac{\partial p}{\partial y}, \quad (4a)$$

$$v = f^{-1}\rho^{-1}\frac{\partial p}{\partial x}, \quad (4b)$$

and finite differencing of the solution for p ($\Delta x = 25$ km, $\Delta y = 10$ km). Each variable has its own response function, although for each case, the maximum response lies at or near the forcing. The pressure response spreads in all directions, but more strongly toward the west. Zonal velocity, u, response is strongest north and south of the driving location but is exactly zero at $y = 0$. This

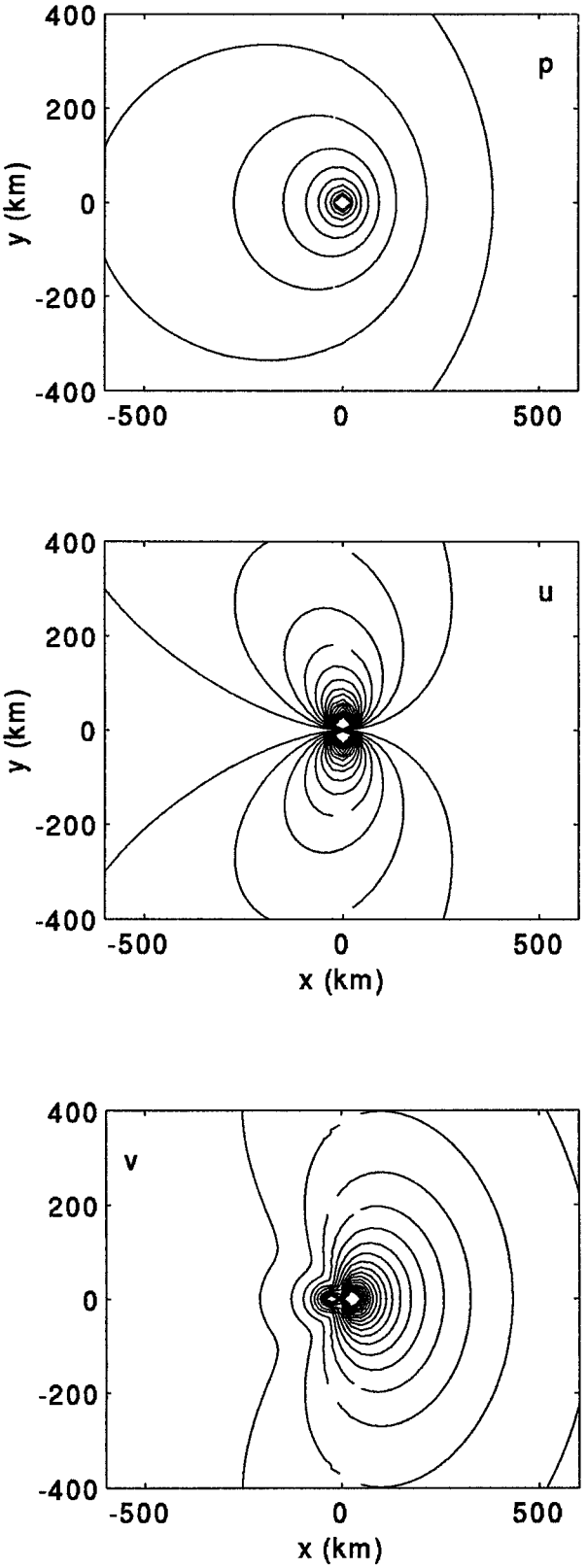

→

FIG. 1. The magnitude of the ocean response to a point forcing at $x = 0$, $y = 0$. Variables shown are pressure, u, and v. Results were calculated using $\beta = 2 \times 10^{-13}$ (cm s)$^{-1}$, $\omega = 1 \times 10^{-6}$ s^{-1}, $\epsilon = 0.05$ cm s^{-1}, and $h = 4000$ m.

response is consistent with the meridional radiation of the short Rossby waves occurring near where the meridional wavenumber magnitude is a maximum. There is also a slight tendency in this case for stronger response toward the west. Finally, meridional velocity, v, response is clearly concentrated to the east of the forcing, dominated by short, eastward propagating Rossby waves.

For the inviscid ($\epsilon = 0$), rigid-lid ($\lambda = 0$) problem (1), there is only one length scale: $\alpha^{-1} = \omega\beta^{-1}$. Scaling (1) using this shows that, as long as friction and divergence are negligible, the response has exactly the same shape regardless of ω and that only the amplitude and scale of the response changes. Adding friction introduces a new parameter, $\epsilon(\omega h)^{-1}$, that can influence the shape of the response as follows: The spindown time for the system is $h\epsilon^{-1}$, and the friction decay distance is

$$L_F = c_g h\epsilon^{-1}, \tag{5a}$$

where c_g is the wave group velocity magnitude. For waves with an eastward component of group velocity ($|k| > 0.5\beta\omega^{-1}$),

$$c_g = O(\omega^2\beta^{-1}), \tag{5b}$$

but longer, westward propagating waves move much faster,

$$c_g \to \infty \quad \text{as} \quad k \to 0. \tag{5c}$$

Thus, eastward propagating waves are much more subject to damping than westward propagating waves. So, as friction increases, the eastward lobe of the v response (Fig. 1) weakens, as do the north and south u lobes. The pressure response becomes more confined to a westward-spreading zonal band with lobes of u response on its edges. Since LM used a substantially larger damping than did Brink (1989), one would expect their Rossby wave responses to have more of a westward bias than Brink's case.

The point of this section is to show that the natural response of a β-plane ocean to an isotropic wind forcing is different for each variable, and not isotropic for any of them (Fig. 1). The v response is felt more to the east, p response more to the west, and u to the north and south. While this simple result is qualitatively useful for thinking about the response to a realistic continuous wind forcing (that could be thought of as a linear superposition of point responses from many locations), it does not translate exactly. The reason is that the observed wind stress curl has more energy at small wavenumbers than at larger ones, so that long, westward propagating Rossby waves will be generated preferentially, thus leading to more of a westward bias in the response pattern than that suggested by Fig. 1.

3. Sources of variance

Model calculations (Brink 1989; Samelson 1990; LM) tend to show maximum coherences between wind stress curl and meridional velocity v for winds near or to the west of the observation point. Similarly, the calculations show coherence maxima for pressure p and zonal velocity u for locations tending to the east of the measurement point. These separations tend to be clearest in what LM call the ''resonant range'' where free Rossby waves are efficiently excited. Brink's (1989) interpretation states that the coherence maxima are indicative of where the predominant wind forcing occurs for a given variable. If this is the case, v should be dominated by energy arriving from the west, and u and p should be dominated by energy coming from the east. This is easy enough to test.

TABLE 1. Fractions of total variance driven from the east (E_4) and west (E_1).

	x_m = 10 000 km		x_m = 100 000 km	
Variable	E_1/E	E_4/E	E_1/E	E_4/E
	15-day period			
p	0.24	0.74	0.08	0.91
u	0.30	0.67	0.15	0.84
v	0.68	0.32	0.62	0.38
	49-day period			
p	2×10^{-4}	1.00	9×10^{-5}	1.00
u	6×10^{-4}	1.01	9×10^{-5}	1.00
v	0.35	0.86	0.09	0.96

The predicted variance E for a given variable is governed by a four-term integral expression [Brink 1989, Eq. (18)] representing the sum of energy coming from the west E_1, energy coming from the east E_4, and two terms (E_2 and E_3: often much smaller) representing interference of the eastward and westward moving energy. It is straightforward to evaluate each of these contributions separately. If all variables were forced at the same location, then E_1/E, for example, would be the same for u, v, and p. Different forcing locations for different variables would likely lead to E_1/E differing for u, v, and p. Likewise, if a variable is driven more to the east than the west, then $E_4 > E_1$.

As an example, consider an unbounded barotropic ocean with wind stress forcing applied over the region $-x_m \le x \le x_m$ (where x_m = 10 000 km) and unbounded in y. We ask about the sources of variance at $x = 0$, so the total variance E, as well as the western E_1 ($x < 0$) and eastern E_4 ($x > 0$) contributions, are computed. Results (first two columns, Table 1) are presented in terms of E_1/E and E_4/E. Note that E need not equal the sum of E_1 and E_4, depending on the contribution to E of the interference terms E_2 and E_3. These terms occur as a complex conjugate pair. Although they are generally small (as can be seen from adding columns of Table 1) they can be nonnegligible in cases where coherence is a maximum near the observation point. Calculations are done using parameters in Brink (1989): Coriolis parameter $f = 6.83 \times 10^{-5}$ s^{-1}, $\beta = 2.02 \times 10^{-13}$ cm^{-1} s^{-1}, meridional inverse squared coherence scale $s = 4.33 \times 10^{-16}$ cm^{-2}, zonal inverse squared scale $\sigma = 2.03 \times$

10^{-16} cm^{-2} (for 15-day period), and $s = 1.81 \times 10^{-16}$ cm^{-2}, $\sigma = 1.84 \times 10^{-17}$ cm^{-2} (for 49-day period).

The results show that different model variables are driven by wind forcing in different parts of the ocean, and in a manner consistent with the coherence maps [see, e.g., Brink (1989) Figs. 11 and 13 for comparison]. Pressure p and zonal velocity u are driven mainly by winds east of the measurement site, especially at the shorter period. Meridional velocity v is driven mainly west of the site at a 15-day period, but more east of the site (but much less so than for u) at 49 days. Thus, the ''notion that variance in the pressure field and velocity field at the same location is generated at different distant locations'' is not ''awkward'' (LM, p.121), but a natural consequence of the fact that, in a linear quasigeostrophic model, the responses of u and v to a given forcing spectrum are effectively weighted relative to the response of p by the meridional and zonal wavenumbers, respectively. As in section 2, the result is simply a statement that, in the resonant range, westward propagating long Rossby waves dominate u and p, while eastward propagating short waves are more important for v.

It is instructive to investigate how the results change with the size of the basin. The above calculations are repeated using $x_m = 100\,000$ km, and results appear in the last two columns of Table 1. Two differences from the previous case are evident. First, all of the variables have a stronger tendency to be driven by winds east of the mooring; that is, E_4 is larger than before. This result makes sense in light of the discussion of frictional decay in section 2 since westward propagating waves are only weakly damped and eastward propagating waves are much more strongly damped. This means that, as the ocean basin becomes larger, increasingly distant forcing to the east can play a role, but forcing at the same distance to the west is unlikely to be felt. A second effect of the larger basin is that the interference terms are relatively less important; that is, $(E_1 + E_4)E^{-1}$ more nearly adds to unity. This follows since the interference terms reflect forcing near $x = 0$, and this relatively local effect should become less important when the overall energy levels increase due to added remote forcing.

These results tend to emphasize how important dissipation is in this problem. If there were no damping, energy could travel infinite distances, albeit with different speeds. A given location would be subject to unattenuated influences from all over the ocean. Once friction enters, however, longer Rossby waves propagate more freely than shorter waves and (except for the effectively undamped strictly westward propagating waves), substantial energy can only be received from some finite distance away. We now have E_1 (short waves) $< E_4$ (long waves) for u, p, and sometimes v. Meridional velocity is anomalous in that it is most efficiently generated by strongly damped eastward propagating waves, but the eastward propagating signal can be dominated by the v associated with the greater amount of westward propagating waves.

For a continuous wavenumber spectrum of forcing in a frictionless unbounded ocean, one would expect to have wind curl–current coherence zero everywhere. This follows because equal amounts of energy arrive at a given point from an infinity of regions, each being incoherent with the others. When dissipation is added, a lesser number of forcing locations enter and coherences will be nonzero, allowing the coherence map to achieve structure. This structure for a given variable will depend upon the statistical properties of the wind, the relevant wave propagation direction (section 2), and damping. For example, if the amplitude of the forcing increases northward, there will be a corresponding northward bias in the coherences, reflecting the dominance of waves forced north of the mooring over waves forced south of the mooring (Samelson and Shrayer 1991).

It is interesting to note the consistency of the overall theoretical results with the observational spectral estimates of Chave et al. (1992). Specifically, they found differing wavenumber spectra for u and v in the northeast Pacific Ocean. Spectral peaks for u occurred at longer zonal wavelengths than for v. As a consequence, the u spectra are consistent with a pseudowestward Rossby wave energy propagation toward the moorings, while the v spectra are consistent with pseudoeastward propagation.

4. The role of the group velocity

We argue here that, for forcing frequencies in the resonant range, the Rossby wave group velocity enters the problem in a physically illuminating way. For this purpose, consider the expression [derived, e.g., from LM Eqs. (10), (13), and (20), modified to include a free surface] for the cross-spectrum between wind stress curl and pressure at a separation $\mathbf{r}$,

$$P_{cp}(\omega, \mathbf{r}) = \iint e^{-i\mathbf{k}\cdot\mathbf{r}} \frac{i}{B(\omega - i\epsilon, \mathbf{k})} |F(\omega, \mathbf{k})|^2 \, dk \, dl, \tag{6}$$

where ω is the frequency, $\mathbf{k}$ the vector wavenumber, κ the scalar wavenumber, $|F|^2$ the frequency–wavenumber spectrum of the forcing, $B(\omega, \mathbf{k})$ the Rossby wave dispersion relation

$$B(\omega, \mathbf{k}) = \omega(\kappa^2 + \lambda^2) + \beta k, \tag{7}$$

k and l are the east and north wavenumber components, $\mathbf{r}$ is the location vector, ϵ is a friction parameter, and λ is a free surface parameter:

$$\lambda^2 = \frac{f^2}{gh} \tag{8}$$

(where g is the acceleration due to gravity and h is the water's depth). Lighthill (1978) has discussed the interpretation of integrals similar to this: we follow his example.

The problem is easiest to consider in a one-dimensional (east–west) case, where the double integral reduces to a single contour integral over k with $l = 0$. The poles of the integral occur at the poles of the spectrum and of the dispersion relation B. If ω is in the resonant range, the latter poles occur at $k = k_0$, where k_0 is real and $B(\omega, k_0) = 0$, or

$$k_0^2 + \frac{\beta}{\omega}k_0 + \lambda^2 = 0, \tag{9}$$

when friction vanishes ($\epsilon = 0$). For small friction (ϵ small), the poles k_ϵ of B in (6) may be estimated by a Taylor expansion,

$$\begin{aligned} 0 &= B(\omega - i\epsilon, k_\epsilon) \\ &\cong B(\omega, k_0) - i\epsilon\frac{\partial B}{\partial \omega} + \frac{\partial B}{\partial k}(k_\epsilon - k_0). \end{aligned} \tag{10}$$

Since $B(\omega, k_0) = 0$ and

$$c_g = \frac{d\omega}{dk} = -\frac{\partial B/\partial k}{\partial B/\partial \omega}, \tag{11}$$

where c_g is the group velocity [evaluated at (ω, k_0)], we obtain

$$k_\epsilon = k_0 - i\epsilon\left(\frac{d\omega}{dk}\right)^{-1} = k_0 - i\epsilon/c_g. \tag{12}$$

That is to say that the poles are displaced from the real axis by an amount proportional to the damping and inversely proportional to the group velocity.

For our example, the two inviscid roots are

$$k_0^{(1)} = -\frac{\beta}{2\omega}\left[1 + \left(1 - \frac{4\omega^2\lambda^2}{\beta^2}\right)^{1/2}\right] \cong -\frac{\beta}{\omega} \tag{13a}$$

and

$$k_0^{(2)} = -\frac{\beta}{2\omega}\left[1 - \left(1 - \frac{4\omega^2\lambda^2}{\beta^2}\right)^{1/2}\right] \cong -\frac{\omega\lambda^2}{\beta}, \tag{13b}$$

where the approximate values are valid for $4\omega^2\lambda^2\beta^{-2} \ll 1$. The corresponding approximate group velocities are, for the short wave $k_0^{(1)}$,

$$c_g^{(1)} \cong \frac{\omega^2}{\beta} \tag{14a}$$

and, for the long wave $k_0^{(2)}$,

$$c_g^{(2)} \cong -\frac{\beta}{\lambda^2}, \tag{14b}$$

corresponding to eastward and westward energy propagation, respectively. Thus

$$k_\epsilon^{(1)} \cong k_0^{(1)} - i\frac{\epsilon}{c_g^{(1)}} \tag{15a}$$

and

$$k_\epsilon^{(2)} \cong k_0^{(2)} - i\frac{\epsilon}{c_g^{(2)}}. \tag{15b}$$

If we choose an ensemble-averaged curl–curl autocovariance of the form

$$S_{cc'}(\omega, r) = b(\omega)e^{-\sigma|r|}, \tag{16}$$

then

$$|F(\omega, k)|^2 = b(\omega)\frac{2\sigma}{\sigma^2 + k^2}, \tag{17}$$

and it is straightforward to evaluate the integral (6) using the residue theorem. The signs of the group velocities determine that the first pole enters for $r > 0$ (for which the contour must be closed in the lower half-plane) and the second pole for $r < 0$ (contour closed in the upper half-plane). For $r < 0$ (westward propagation) we obtain for the cross-spectrum

$$S_{cp}^{-}(\omega, r) = a\exp(-ik_0^{(2)}r - \epsilon r c_{g_2}^{-1}) + d\exp(\sigma r), \tag{18a}$$

where

$$a = 4\pi b(\omega)\sigma[(\omega - i\epsilon)(k_\epsilon^{(1)} - k_\epsilon^{(2)})(\sigma^2 + k_\epsilon^{(2)2})]^{-1}, \tag{18b}$$

$$d = 2\pi i b(\omega)[(\omega - i\epsilon)(\lambda^2 - \sigma^2) + i\beta\sigma]^{-1}, \tag{18c}$$

and a similar expression is obtained for $r > 0$. Finally, it is straightforward [LM Eq. (42b)] to obtain expressions for the cross-spectrum between wind curl and northward velocity $S_{cv}^{\pm}$:

$$S_{cv}^{\pm} = \frac{\partial}{\partial r}S_{cp}^{\pm}, \tag{19}$$

while the zonal velocity is identically zero. The cross-spectrum (18a) shows that the group velocity enters the problem in a natural way. It expresses the tendency for energy to propagate away from the forcing location to the observation point, thus helping to set the location of the coherence maximum.

Expression (18) provides a convenient basis to calculate how far away the maximum coherence between wind stress curl and pressure occurs. This happens when $|S_{cp}|$ is maximized with respect to separation r (since S_{cc} and S_{pp} are independent of r). The dependence of this distance on the group velocity may be shown explicitly by solving the maximization problem analytically in an accessible limit. Suppose ω and λ are such that $k_0^{(2)^2} \ll \sigma^2$, $\lambda^2 \ll \sigma^2$, $\sigma^2 \ll \beta^2/\omega^2$. That is to say that the forcing length scales are short relative to long Rossby waves and the barotropic Rossby radius, but not relative to short Rossby waves. Then

$$a \cong -\frac{4\pi}{\beta\sigma}b(\omega), \qquad d \cong \frac{2\pi}{\beta\sigma}b(\omega) \cong -\frac{1}{2}a,$$

and

$$|S_{cp}^{(-)}|^2 \cong |a|^2\left[e^{-2\epsilon r/c_g^{(2)}} + \frac{1}{4}e^{2\sigma r} - e^{(\sigma-2\epsilon/c_g^{(2)})r}\cos(k_0^{(2)}r)\right]. \tag{20}$$

Suppose also that $|\epsilon/c_g^{(2)}| \ll \sigma$. Then

$$\left(\frac{d}{dr}|S_{cp}^{(-)}|^2\right)\bigg|_{r=0} \cong -\frac{1}{2}\sigma|a|^2 < 0,$$

so the coherence increases away from the origin toward negative r. Since $|S_{cp}^{(-)}|^2 \to 0$ as $r \to -\infty$, there must exist a relative maximum in $-\infty < r < 0$. If the most rapidly decaying term (the second term) in (20) is neglected, then the condition

$$\frac{d}{dr}|S_{cp}^{(-)}|^2 = 0 \quad \text{at } r = r_m$$

may be solved to obtain the separation r_m of maximum coherence,

$$r_m \cong \frac{1}{\sigma}\ln\left(\frac{-2\epsilon}{\sigma c_g^{(2)}}\right). \tag{21}$$

An analogous result was obtained by Allen and Denbo (1984). The presence of the group velocity $c_g^{(2)}$ in this expression explicitly links the physical mechanism of wave group propagation to the appearance of the remote coherence maximum.

The result (21) again emphasizes the role of damping in determining coherence maps. As $\epsilon \to 0$, the location of the coherence maximum becomes more remote from the observation point. Decreased damping is also associated with a lowered maximum coherence. This coherence reduction is mentioned briefly in Brink (1989), and in detail by Allen and Denbo (1984), but is not obvious from (20) because coherence is partly determined by the autospectrum of the response variable. This autospectrum will tend to grow as friction decreases. These mathematical arguments can be interpreted to imply that enhanced damping leads to weaker but increasingly localized responses. Within this smaller domain, coherences at a given location can increase because the fraction of driving from a given region of coherent winds increases. In the limit of $|c_g^{(2)}\epsilon^{-1}| \ll \sigma^{-1}$, the damping length scale is shorter than the wind coherence scale, so all forcing felt at a point will be coherent with the local wind: coherence should approach unity.

5. Conclusions

Our main point is in regard to the physical interpretation of theoretical results for wind-driven barotropic currents. LM suggest that the coherence maxima between forcing and response are a mathematical artifact, that different variables observed at one place cannot be primarily driven at differing locations, and that energy propagation with the group velocity plays no role in their solutions. We have demonstrated that, due to the anisotropy of β-plane flow, different oceanic variables can indeed be forced in different regions. Further, we have demonstrated how the group velocity enters the problem for forcing frequencies in the resonant range and so participates in setting the location of coherence maxima.

We caution the reader that the one- or two-wave examples provided by Müller and Lippert (1998) should be interpreted with caution. For a simpler example, consider the equation governing long coastal-trapped waves (Allen and Denbo 1984)

$$c^{-1}Y_t + Y_y + (cT_F)^{-1}Y = B\tau^y(y, t), \tag{22}$$

where Y is a modal amplitude, c is the constant phase speed (>0), T_F is a frictional decay time, B is a coupling coefficient, and τ^y is the alongshore wind stress. In this case, energy can propagate only toward positive y, so at a given location y_0 only forcing at $y < y_0$ contributes. Nonetheless, forcing by a single sinusoid will lead to a $Y - \tau^y$ coherence of unity everywhere, and forcing by a pair of sinusoids yields the same ''beating'' pattern demonstrated by Müller and Lippert (1998) for the more complex midocean problem. These patterns of high coherence over all space (due to the coherence of forcing with itself not decaying) are clearly inconsistent with the physical content of (22) even though they are mathematically correct. For the case of (22), it is only when a continuum of forcing sinusoids is applied that one obtains the physically informative result of maximum $Y - \tau^y$ coherence at some $y < y_0$ (see Allen and Denbo 1984). We expect that one must be similarly cautious with overly simplified forcing in the β-plane case.

The theoretical coherences calculated above and by Brink (1989) are ensemble-averaged quantities that depend on the assumed statistical properties of the forcing field and, so, are intrinsically nonlocal and nondeterministic. Nonetheless, the coherence maxima may be interpreted as the locations of most effective forcing, in the following sense. Suppose for each realization of the ensemble, the response at the mooring to forcing at a fixed frequency is calculated separately for forcing at each point of the domain (as in section 2). Since each of these calculations is linear and deterministic, the forcing and response will be perfectly correlated in each. The coherence statistics may be obtained by ensemble averaging over all of these realizations. The location of maximum coherence is that point for which the ensemble-averaging degrades the correlation between local forcing and response at the mooring by the minimal amount, that is, the point where the deterministic relation between local forcing and remote response is least affected by interference from the response to uncorre-

lated (random-phase) forcing at other locations. It should be clear that this does not imply that the response at the mooring is dominated by forcing near the coherence maximum, unless the coherence at the maximum is near unity. That is, when maximum coherences are low, even the locations of the most effective forcing are relatively inefficient.

Acknowledgments. We wish to thank Alan Chave for useful comments. This effort was supported by the Office of Naval Research, Coastal Sciences code (Grant N00014-92-J-1528 for KB) and the National Science Foundation (NSF OCE94-15512 for RS).

REFERENCES

Allen, J. S., and D. W. Denbo, 1984: Statistical characteristics of the large-scale response of coastal sea level to atmospheric forcing. *J. Phys. Oceanogr.,* **14,** 1079–1094.

Bendat, J. S., and A. G. Piersol, 1971: *Random Data: Analysis and Measurement Procedures.* Wiley-Interscience, 407 pp.

Brink, K. H., 1989: Evidence for wind-driven current fluctuations in the western North Atlantic. *J. Geophys. Res.,* **94,** 2029–2044.

Chave, A. D., D. S. Luther, and J. H. Filloux, 1992: The barotropic electromagnetic and pressure experiment. Part 1. Barotropic current response to atmospheric forcing. *J. Geophys. Res.,* **97,** 9565–9593.

Frankignoul, C., and P. Müller, 1979: Quasi-geostrophic response of an infinite β-plane ocean to stochastic forcing by the atmosphere. *J. Phys. Oceanogr.,* **9,** 104–127.

Lighthill, J., 1978: *Waves in Fluids.* Cambridge University Press, 504 pp.

Lippert, A., and P. Müller, 1995: Direct atmospheric forcing of geostrophic eddies. Part II: Coherence maps. *J. Phys. Oceanogr.,* **25,** 106–121.

Müller, P., and A. Lippert, 1998: Reply. *J. Phys. Oceanogr.,* **28,** 1010–1013.

Samelson, R. M., 1989: Stochastically forced current fluctuations in vertical shear and over topography. *J. Geophys. Res.,* **94,** 8207–8215.

——, 1990: Evidence for wind-driven current fluctuations in the eastern North Atlantic. *J. Geophys. Res.,* **95**(C7), 11 359–11 368.

——, and B. Shrayer, 1991: Currents forced by stochastic winds with meridionally-varying amplitude. *J. Geophys. Res.,* **96**(C10), 18 425–18 429.